ELSEVIER

Thermochimica Acta 377 (2001) 193–204

thermochimica acta

www.elsevier.com/locate/tca

Simultaneous multi-frequency TMDSC measurements

M. Merzlyakov*, C. Schick

Department of Physics, University of Rostock, Universitätsplatz 3, 18051 Rostock, Germany

Received 18 January 2001; received in revised form 25 March 2001; accepted 28 March 2001

Abstract

We presented a study of advantages and limitations of different temperature–time profiles for simultaneous multi-frequency TMDSC measurements. Theoretical consideration was followed by some experimental examples. We showed that the optimal program temperature should contain sharp steps. In experiments higher harmonics of heat flow rate up to 100th were detected which means simultaneous covering two decades of frequency in a single measurement. Importance of linear conditions was also discussed and the way to check linearity was shown. © 2001 Elsevier Science B.V. All rights reserved.

Keywords: Dynamic heat capacity; Higher harmonics; Heat capacity spectrum; TMDSC; Linear response

1. Introduction

In spite of the fact that the first temperature modulated differential scanning calorimeter (TMDSC) was made by Gobrecht et al. [1] to measure frequency dependence of dynamic heat capacity, the technique was widely introduced by Reading [2] to deconvolute the total heat flow signal into the non-rapidly reversing and the rapidly reversing parts. Further research and practice with TMDSC showed the usefulness of measurements at different frequencies of temperature modulation. Having the frequency dependence of complex heat capacity c_p^* (other terms are: dynamic, apparent, effective heat capacity; reversing heat capacity for modulus of c_p^*) one can study, e.g. dynamic glass transition [3], kinetics of irreversible processes [4], dynamics of reversible melting [5,6]. Even when heat capacity of the material is frequency independent one can get precise heat capacity values studying the frequency dependence of measured c_p^* [7].

One way to improve the technique in respect to heat capacity spectroscopy is to measure c_p^* simultaneously at different frequencies. This would ensure an exact correspondence of the sample history for all frequencies. Multi-frequency measurement can be realized by looking at the spectrum of higher harmonics of the heat flow rate under inharmonic temperature perturbations. Inharmonic perturbations can be programmed as common saw-tooth. The application of this temperature profile to multi-frequency measurements is analyzed in [8]. Since the temperature amplitude of higher harmonics of a saw-tooth is inversely proportional to the square of harmonic number, the heat flow rate decreases very fast at higher harmonics resulting in a low signal-to-noise ratio. Wunderlich et al. [7] suggested another type of inharmonic periodic temperature–time profile, a complex saw-tooth, which has first four even harmonics with the same temperature amplitude and consist of 14 linear heating/cooling segments per period.

The goal of the present paper is to analyze which temperature–time profile is optimal for simultaneous

* Corresponding author. Tel.: +49-381-498-1616; fax: +49-381-498-1626.
E-mail address: mikhail.merzliakov@physik.uni-rostock.de (M. Merzlyakov).

0040-6031/01/$ – see front matter
PII: S0040-6031(01)00554-8

multi-frequency TMDSC measurements and to show which results can be achieved by applying that temperature–time profile. We start our study from analyzing the TMDSC data treatment to point out two important theoretical prerequisites for dynamic heat capacity calculations: linear and stationary response and the presence of components at the frequency under investigation in the input signal (temperature). Next, in Section 3, we analyze two limiting factors with regard to the experimental determination of dynamic heat capacity: noise level and non-linear response. Larger temperature amplitudes guarantee better signal-to-noise ratio but can bring the instrument and the sample beyond linear response. It is important to find out the optimal experimental conditions for heat capacity measurements. We present a multi-frequency method where the experimental parameters are selected in an optimal way for simultaneous dynamic heat capacity measurement at different frequencies. After that, in Section 4, we show how to check linearity of the thermal response. Further we select experimental conditions (temperature amplitude) based on the results of this linearity check to perform real measurements in glass transition and melting region, which are shown in Section 5. Finally, in Section 6, we analyze whether the proposed multi-frequency method gives the expected results, what are the advantages of the method with respect to classical TMDSC.

2. Data treatment

Let us consider where heat capacity spectrum comes from. To answer this question let us go one step back and consider how heat capacity is calculated. Heat capacity C of a system is introduced as the ratio between the elementary amount of heat $\mathrm{d}Q$ added to the system to respective temperature change $\mathrm{d}T$,

$$C = \frac{\mathrm{d}Q}{\mathrm{d}T} \tag{1}$$

One can formally rewrite this equation as

$$C = \frac{\mathrm{d}Q/\mathrm{d}t}{\mathrm{d}T/\mathrm{d}t} = \frac{\mathrm{HF}}{q} \tag{2}$$

where $\mathrm{HF} = \mathrm{d}Q/\mathrm{d}t$ is the heat flow rate to the system and $q = \mathrm{d}T/\mathrm{d}t$ is the heating rate. This is the way in which standard differential scanning calorimeters (DSC) calculate heat capacity, see e.g. [9]. However, Eq. (2) gives the same heat capacity C as Eq. (1) only when one gives enough time for all subsystems to reach equilibrium. In general case, with remarkable heat transfer delay and/or relaxations in the material, the relation between HF and q is not simply proportional, $\mathrm{HF} = C \times q$, but it is given by the operator equation

$$\mathrm{HF}(t) = \hat{C}q(t) \tag{3}$$

where the operator $\hat{C}$ transfers a set of functions $q(t)$ to a set of functions $\mathrm{HF}(t)$ and may depend on starting temperature T_0 and starting time t_0 of the experiment. If the operator $\hat{C}$ is linear and stationary one can rewrite Eq. (3) as the convolution product

$$\mathrm{HF}(t) = C(t) * q(t) \tag{4}$$

where $C(t)* = \hat{C}$. To resolve the convolution product one selects a periodic function for $q(t)$ and applies Fourier transformation, e.g. in the following form:

$$F[f(t)](\omega) \equiv A_f(\omega) = \frac{2}{t_\mathrm{p}} \int_{-t_\mathrm{p}/2}^{t_\mathrm{p}/2} f(t)\cos(\omega t)\,\mathrm{d}t + \mathrm{i}\frac{2}{t_\mathrm{p}} \int_{-t_\mathrm{p}/2}^{t_\mathrm{p}/2} f(t)\sin(\omega t)\,\mathrm{d}t \tag{5}$$

where $F[f(t)](\omega)$ is the Fourier image of the function $f(t)$ on frequency ω, another name for that is "complex amplitude" $A_f(\omega)$, $\omega = 2\pi/t_\mathrm{p}$, t_p is the period of the function $f(t)$. Applying Fourier transform one can rewrite Eq. (4) as regular product:

$$F[\mathrm{HF}(t)](\omega) = F[C(t)](\omega) \times F[q(t)](\omega) \quad \text{or} \quad A_\mathrm{HF}(\omega) = C(\omega) \times A_q(\omega) \tag{6}$$

Then the heat capacity at given frequency $C(\omega)$ (complex value) is determined as follows:

$$C(\omega) = \frac{A_\mathrm{HF}(\omega)}{A_q(\omega)} \tag{7}$$

Note that one cannot determine heat capacity analogous way in time domain, because the value $C(t)$, $C(t) = \mathrm{HF}(t)/q(t)$, would depend on the whole profile of the function $q(t)$, that assumes infinite number of parameters being involved in the analysis. In contrary $C(\omega)$ depends only on frequency ω and on starting temperature. Thus, heat capacity spectrum gives

almost all information which one can get from the analysis of heat flow rate HF(t) and heating rate $q(t)$.

The only limitation of applying Fourier transformation is that the response of the system must be linear and stationary, see [10] for details. Stationary response assumes that the relation between heating rate $q(t)$ and heat flow rate HF(t) does not change with time and linear response assumes that the heat flow rate proportionally changes with changing heating rate, i.e. $\hat{C}\alpha q(t) = \alpha C q(t)$ for any complex number α.

We discuss experimental data in terms of effective (apparent) specific heat capacity, i.e. $c_{\mathrm{eff}}(\omega) = C(\omega)/m_{\mathrm{s}}$ where m_{s} is sample mass. This specific heat capacity value is not necessarily a material property but we use it for easier comparison on graphs.

Let us assume further that for some periodic heating rate $q(t)$ our instrument has such sampling rate, that we get n points per period for HF(t) and $q(t)$ signals. If one is interested only in the value of $c_{\mathrm{eff}}(\omega)$ then it is not necessary to determine separately $A_{\mathrm{HF}}(\omega)$ and $A_q(\omega)$ in Eq. (7), one can directly calculate $c_{\mathrm{eff}}(\omega)$ omitting all normalization factors:

$$c_{\mathrm{eff}}(\omega) = \frac{1}{m_{\mathrm{s}}} \frac{\sum_{i=1}^{n} \mathrm{HF}_i \cos(\omega t_i) + \mathrm{i}\sum_{i=1}^{n} \mathrm{HF}_i \sin(\omega t_i)}{\sum_{i=1}^{n} q_i \cos(\omega t_i) + \mathrm{i}\sum_{i=1}^{n} q_i \sin(\omega t_i)} \tag{8}$$

The points HF_i and q_i should be taken with the same sampling rate (number of points per unit time) and equidistant. This way of calculating complex $c_{\mathrm{eff}}(\omega)$ is preferable also because there is no need to take care for initial phase of $A_{\mathrm{HF}}(\omega)$ and $A_q(\omega)$.

One should pay attention on the sign of the imaginary part of $c_{\mathrm{eff}}(\omega)$. By tradition one write complex frequency dependent heat capacity in form $C^*(\omega) = C'(\omega) - \mathrm{i}C''(\omega)$ or $C^*(\omega) = |C^*|\mathrm{e}^{-\mathrm{i}\varphi}$. The delay in the response due to relaxation processes causes some positive peak in imaginary part C'' as well as in the phase angle φ. However, actual phase angle between heating rate and heat flow rate should be negative if calculated by Eq. (8). If one wish to follow traditional way one should take conjugate value of $c_{\mathrm{eff}}(\omega)$ or calculate $c_{\mathrm{eff}}(\omega)$ as

$$c_{\mathrm{eff}}(\omega) = \frac{1}{m_{\mathrm{s}}} \frac{\sum_{i=1}^{n} \mathrm{HF}_i \cos(\omega t_i) - \mathrm{i}\sum_{i=1}^{n} \mathrm{HF}_i \sin(\omega t_i)}{\sum_{i=1}^{n} q_i \cos(\omega t_i) - \mathrm{i}\sum_{i=1}^{n} q_i \sin(\omega t_i)} \tag{9}$$

In further examples we presented the data of modulus and argument of $c_{\mathrm{eff}}(\omega)$, calculated by Eq. (9).

To apply Fourier transformation we should have a periodic signal in heating rate (under stationary response we get automatically periodic heat flow rate as well). Usually one tends to use the simplest periodic function — sinusoid. In this case $A_q(\omega) \neq 0$ only at the basic frequency ω_0 and we get only one point in the spectrum of $c_{\mathrm{eff}}(\omega)$. However, from the theory nothing is said about the shape of the input signal. It can be any periodic function with the only limitation, that $A_q(\omega)$ could not equal zero, see Eq. (7). Therefore, we can add some higher harmonics to the sinusoidal heating rate and measure them simultaneously at the same time. One can add any frequency $\omega = k\omega_0$ as long as k is integer without changing the basic period of the resulting signal. In fact it is not necessary to program all higher harmonics of interest, it is enough to take some non-harmonic periodic heating rate profile and to analyze the higher harmonics it has. So which profile is the better one for real measurements?

3. Favorable generation of the heat capacity spectrum

3.1. Noise level

Real measurements are always accompanied by noise. If it is mainly white noise, it has equal contribution at all frequencies. If the measured heat flow rate has the same amplitude at all harmonics then the heat capacity spectrum is determined with about the same uncertainties due to the noise at different

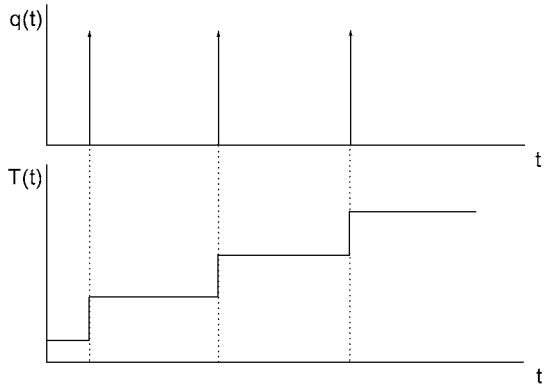

Fig. 1. Heating rate profile consisting of one delta function per period and corresponding temperature–time program.

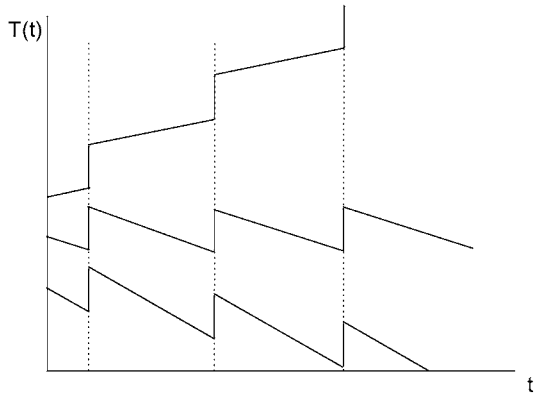

Fig. 2. Temperature–time programs with the same steps in temperature and different underlying heating rates.

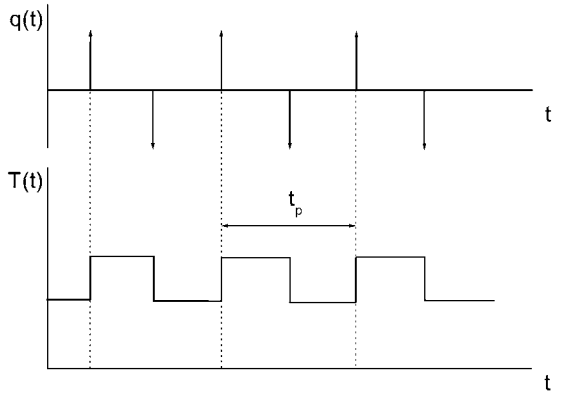

Fig. 4. Heating rate profile consisting of positive and negative delta functions. Temperature–time profile has rectangular shape.

frequencies. Since the amplitude of the heat flow rate is proportional to the heating rate amplitude (not temperature amplitude) an optimal heating rate signal would be one with all higher harmonics of the same amplitude. Such heating rate profile can be generated with one delta function $\delta(t - t_i)$ in heating rate per period, see Fig. 1. The corresponding temperature profile consists of step-wise increasing segments.

Whether one has isotherm or slow heating or cooling between steps in temperature depends on underlying heating or cooling rate, which can be easily added to the temperature–time program, see Fig. 2.

Whenever it is necessary the temperature steps can be negative as well, see Fig. 3.

In all examples above heating rate consists of all even and odd higher harmonics. In contrary, rectangular temperature profile, shown in Fig. 4, has only odd harmonics and no even ones. This gives a possibility to monitoring linearity and stationarity of the response — under linear and stationary conditions even harmonics in the heat flow rate should equal zero, see also Fig. 6.

In the temperature–time diagram we simply connect the steps in temperature by linear heating or cooling segments or by isotherms. Of course one can combine the steps in temperature with any periodic function. But it is the temperature step, which generate a homogeneous heating rate spectrum.

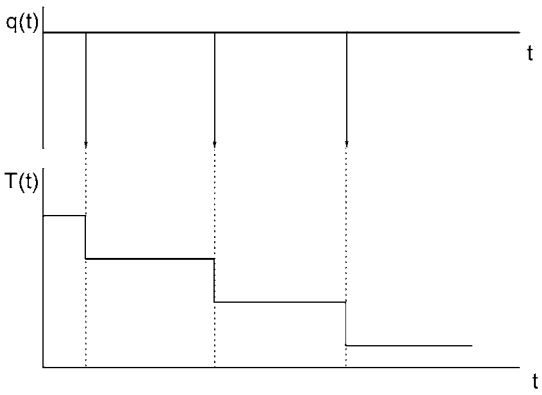

Fig. 3. Heating rate profile consisting of negative delta functions. Temperature–time program has negative steps.

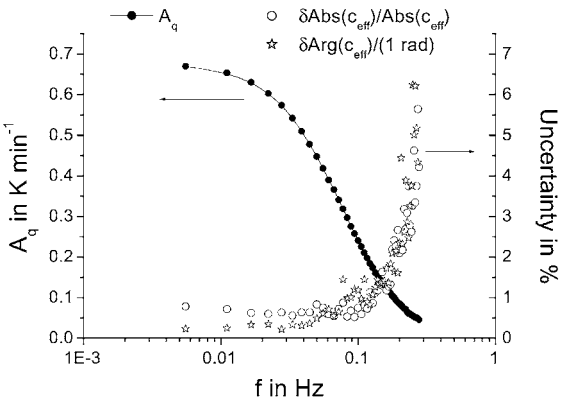

Fig. 5. Measured heating rate amplitude and relative uncertainties in modulus Abs(c_{eff}) and phase angle Arg(c_{eff}) of effective heat capacity, calculated by Eq. (9), vs. frequency for a temperature–time profile consisting of 1 K steps in temperature, period $t_p = 3$ min. Perkin-Elmer Pyris-1 DSC, PS disk of 62 mg.

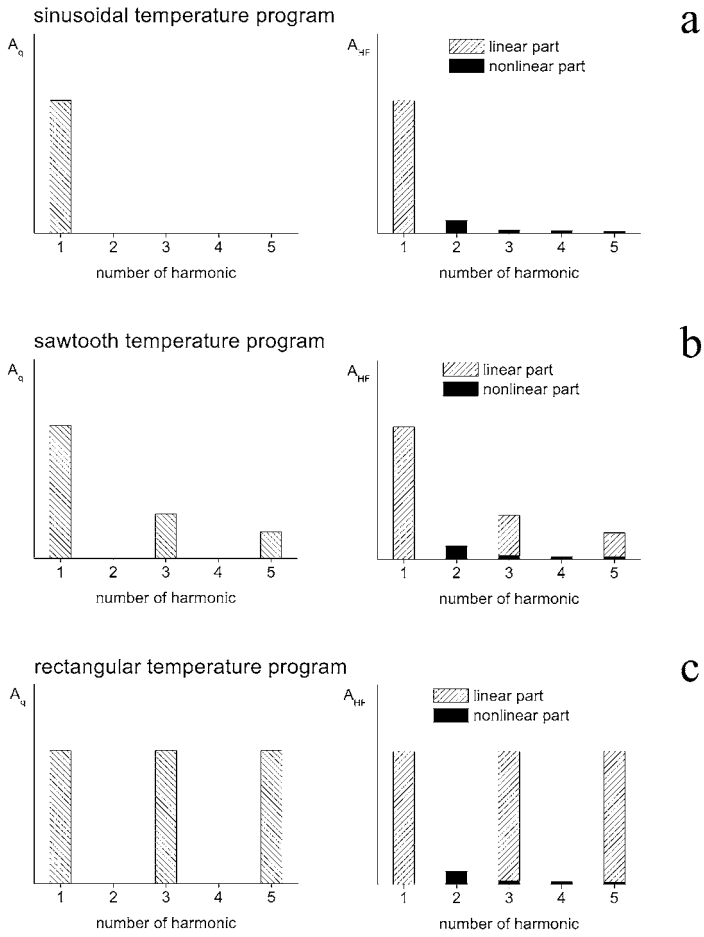

Fig. 6. Schematic representation of heating rate (A_q) and heat flow rate ($A\{_{HF}\}$) spectra for: (a) harmonic temperature perturbations; (b) sawtooth temperature perturbations; (c) rectangular temperature perturbations. The linear part of the $A\{_{HF}\}$ spectrum corresponds to linear response to heating rate perturbations, non-linear part corresponds to harmonic distortions of the response on basic frequency (the values were taken from [11] for 8 K temperature amplitude).

In real measurements, however, measured (real) temperature is smeared by the instrumental lag, which leads to a damping of higher harmonics of the heating rate. Heat transfer and possible time-dependent processes in the sample damp the heat flow rate spectrum in addition.

How uncertain do we measure heat capacity spectrum then? Let us consider the results, shown in Fig. 5. Here we have a heating rate spectrum measured just in the upper limit of the frequency window of the instrument. Instead of constant amplitude of higher harmonics of the programmed heating rate, measured heating rate (that is time derivative of measured temperature) has decreasing amplitude with frequency. In spite of this decrease the uncertainty of heat capacity determination (which comes from signal-to-noise ration in heat flow rate) remains constant up to frequencies of about 0.15 Hz and it is below 1.5% for the modulus and phase of effective heat capacity. Note that at 0.15 Hz the realized heating rate amplitude is already four times lower than that of the basic frequency (5.6 mHz). It means that apparatus damps not only the heat flow spectrum but also the noise spectrum. Further increase of frequency finally leads to decreasing signal-to-noise ratio and uncertainties in heat capacity determination become larger. In the frequency range relevant to classical TMDSC (lower than 0.1 Hz) we have practically the same

signal-to-noise ratio in the heat flow rate for all frequencies.

If we would apply a saw-tooth temperature oscillation instead of temperature steps, heating rate amplitude would decrease with frequency much stronger resulting in higher uncertainties at the high frequency part of the heat capacity spectrum. On the other hand temperature oscillations with increasing heating rate amplitude with frequency would result in higher uncertainties at the low frequency part of the heat capacity spectrum. Only steps in temperature yield the optimal signal-to-noise ratio against other periodic signals.

3.2. Non-linear thermal response

Another and even more important reason to have higher harmonics in the heating rate with the same amplitude is the following. Often the response of the sample to temperature changes is non-linear. In this case under pure sinusoidal temperature oscillations the heat flow rate has already some higher harmonics, e.g. 3% of third harmonic at glass transition with temperature amplitude 8 K [11], see Fig. 6a. If we apply symmetric saw-tooth temperature oscillations where the heating rate amplitude of the third harmonic equals 33% of that of basic frequency, then we get already 10% of the heat flow signal from harmonic distortion, see Fig. 6b. The result would differ for about 10% from that measured separately on this frequency. When perturbing the system with the same heating rate amplitude on the third harmonic as on the first one the response contains only 3% from harmonic distortions, see Fig. 6c. Remember that under non-linear response the first harmonic is already distorted to some extent regardless of the shape of the temperature profile.

We can think about having higher harmonics in heating rate with increasing amplitude. This can be realized for example by having delta functions in temperature profile, or creating some of the harmonics by applying complex saw-tooth temperature profile [7]. But then heat capacity at lower harmonics will be more uncertain than that at higher harmonics, as was already discussed in Section 3.1. Total peak-to-peak periodic temperature changes of such temperature profiles are larger than temperature amplitude of basic harmonic. On the other hand we are not allowed to increase the temperature changes above a given limit because of non-linearity. This means that one cannot use optimal way the given limit of temperature changes, see Fig. 7.

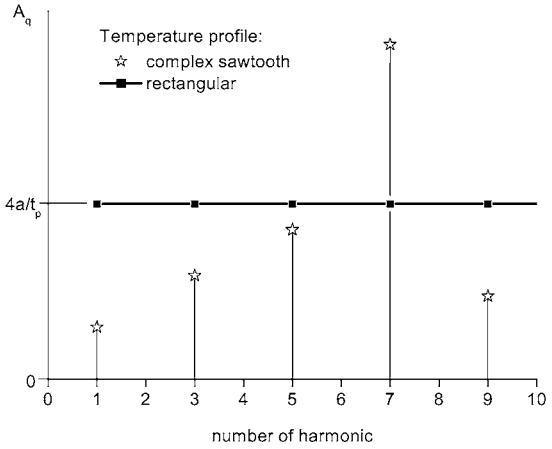

Fig. 7. Schematic representation of heating rate spectrum for rectangular temperature profile (close squares) and for complex saw-tooth (open stars, the values were taken from [7]) at the same peak-to-peak temperature changes a. Complex saw-tooth gives larger A_q value only at 7th harmonic, all others are smaller than that from rectangular temperature profile.

In contrary, if we apply rectangular temperature–time profile, the amplitude of basic harmonic is even larger than total temperature changes, see Fig. 8.

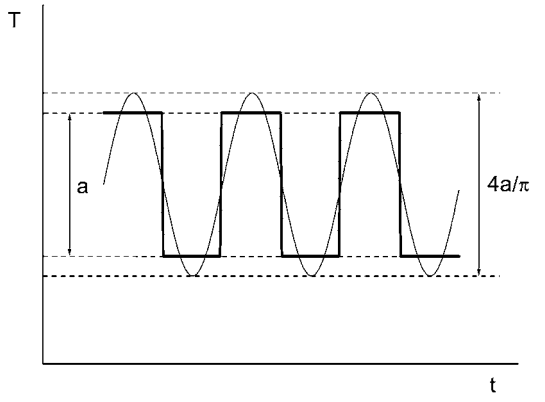

Fig. 8. Rectangular temperature–time profile, which consists of heating and cooling temperature steps. At given limit of temperature changes a the rectangular profile realizes the largest possible peak-to-peak heating rate amplitude $8a/t_p$ (with t_p period), which corresponds to effective temperature oscillations with $4a/\pi$ peak-to-peak amplitude.

Often occurring are the limiting cooling capabilities of the DSC because the instrument at given temperature could not cool faster than certain value $q_{\max}^{\text{cool}}$. In this case heating rate amplitude $A_q \leq q_{\max}^{\text{cool}}$ for quasi-isothermal measurements with sinusoidal temperature oscillations. However, heating capability of the same instrument is much better. Therefore, one can use a periodic temperature profile consisting of sharp heating and slow cooling with $q(t) = q_{\max}^{\text{cool}}$. This way one gets an increasing of heating rate amplitude A_q almost for two times and therefore one doubles the signal-to-noise ratio.

If the instrument cannot realize sharp step-wise changes in temperature then this is an instrument limitation but not a limitation of the method. Then it is impossible to make the instrument react faster by any other temperature–time program.

Consequently, at quasi-linear response the steps in temperature yield optimal signal-to-''harmonic distortion'' ratio against other periodic signals. The question remains: which temperature steps should we use? In general the larger the amplitude the better the signal-to-noise ratio. But this obvious conclusion is not valid under non-linear response, because the harmonic distortions can increase with the amplitude. Then the question arises: under which conditions the response is linear or quasi-linear? To answer the question we have to perform a linearity check.

4. Linearity check

It is worth to repeat once again that multi-frequency method as well as classical TMDSC is only correct when the response of the system (apparatus + sample) is linear and stationary. To decrease non-linearity one should decrease the amplitude of the temperature oscillations. To decrease non-stationarity (instrumental drift, evolution of sample properties) one should shorten the modulation period or/and slow down sample evolution by decreasing underlying heating rate, changing crystallization temperature, etc. [12].

Sometimes one mixes non-linearity with differences in specific heat capacity by measuring different sample masses. In this case the response is not necessarily non-linear. One has the differences because one measures different systems. To get the same specific values is the question of right correction but not of linear response.

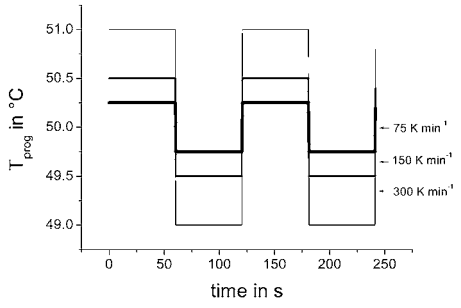

Fig. 9. Temperature–time program for linearity check. The length of each isotherm is 1 min, each heating and cooling segment is 0.4 s, heating and cooling rate is 75, 150 and 300 K min^{-1}, which makes temperature steps of 0.5, 1 and 2 K, respectively. Perkin-Elmer Instruments Pyris-1 DSC, $t_p = 2$ min, block temperature $T_{\text{block}} = -20$°C.

The linearity check in TMDSC has the same importance as calibration of the instrument. To check linearity of the response one can vary the perturbation amplitude, i.e. temperature amplitude, which is applied to the same system. The same system means that sample inside the instrument should not be removed or replaced between subsequent measurements with different temperature amplitudes. In Fig. 9 we have three similar temperature–time programs with different temperature amplitudes.

We took an aluminum disk as the sample, which obviously has linear thermal response at the temperature range of interest. This way we check linearity of the instrument only. The results of $c_{\text{eff}}^{*}(\omega)$ for the three different temperature amplitudes are shown in a Cole–Cole plot, see Fig. 10.

Under linear response conditions $c_{\text{eff}}(\omega)$ should not depend on the modulation amplitude. The values of $c_{\text{eff}}(\omega)$ coincide with each other for 0.5 and 1 K temperature steps. The values of $c_{\text{eff}}(\omega)$ for 2 K temperature steps remarkably deviate from others, especially at higher harmonics (points which are closer to the origin of the coordinates in the complex plane). This means that at given rectangular temperature–time profile the response was linear till peak-to-peak amplitude of 1 K. In this particular case most probably the limiting cooling capabilities of the instrument caused the non-linearity at 2 K peak-to-peak amplitude.

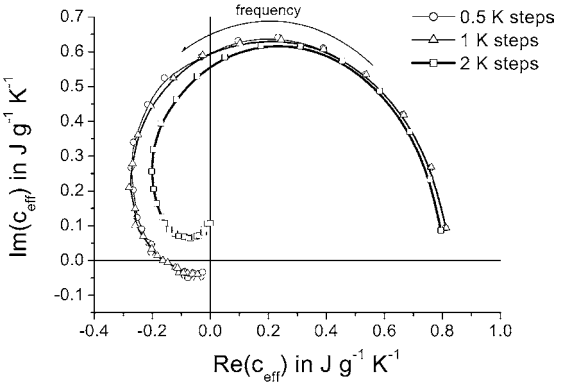

Fig. 10. Cole–Cole plot of $c_{\mathrm{eff}}(\omega)$ with frequency as a parameter for three different temperature amplitudes. The horizontal and vertical axes show the real and imaginary parts of $c_{\mathrm{eff}}(\omega)$, respectively. Perkin-Elmer Pyris-1 DSC, aluminum disk of 16 mg. Experimental conditions as in Fig. 9.

We performed analogous linearity check (by varying temperature amplitude) with temperature–time profiles consisting of cooling steps only and heating steps only. Cooling steps up to 1 K height and heating steps of 2 K height did not violate the linearity of instrumental response.

5. Experimental results

Here we present three types of multi-frequency measurements: cooling steps, heating steps and rectangular profile consisting of heating and cooling steps. The step height was selected taking care not to violate linear response conditions.

5.1. Glass transition of polystyrene

The following example shows how broad can be the spectrum of complex heat capacity, calculated from a single run.

The 168 N polystyrene (PS) sample was from BASF ($\rho = 1.047\ \mathrm{g\ cm^{-3}}$; $M_{\mathrm{n}} = 95{,}000\ \mathrm{g\ mol^{-1}}$; $M_{\mathrm{w}} = 270{,}000\ \mathrm{g\ mol^{-1}}$). The temperature–time profile was programmed by repeating of two segments: isotherm and fast cooling. The duration of the isotherm was 10 min and the cooling step was 1 K high (to keep linear instrumental response) with 30 K $\mathrm{min^{-1}}$ cooling rate that makes a duration of the cooling segment

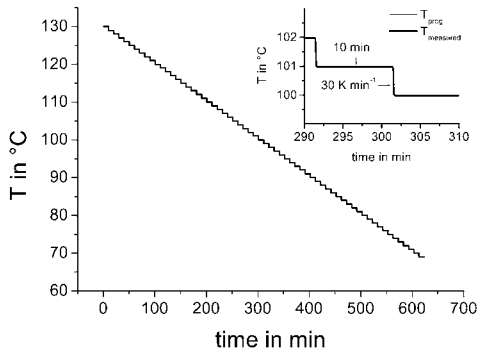

Fig. 11. Temperature–time profile, consisting of repetition of isotherm-cooling segments. Perkin-Elmer Instruments Pyris-1 DSC. Insert shows closer view on two periods.

of 2 s. The whole temperature–time profile is shown in Fig. 11. The insert shows the program temperature T_{prog} and the measured sensor temperature (called "sample temperature" in Pyris$^{\mathrm{TM}}$ software) T_{measured} for two periods. One can see that in this temperature–time scale measured temperature follows very tightly program temperature.

Fig. 12 shows the measured heat flow rate of a sample run after subtraction of the baseline heat flow rate. The very sharp negative peaks correspond to the very short cooling segments with high cooling rate. One can see by eye that the peaks height became

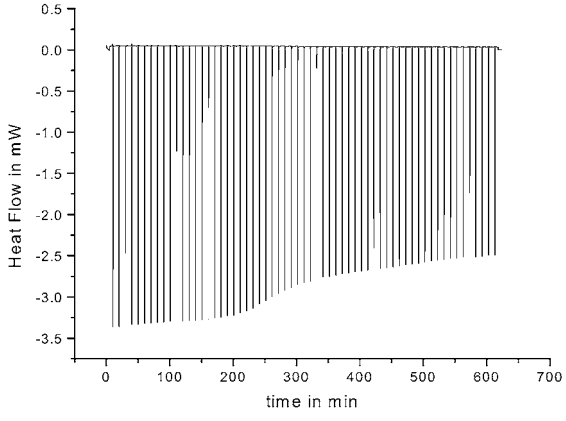

Fig. 12. Heat flow rate vs. time which corresponds to temperature–time program, shown in Fig. 11. Perkin-Elmer Instruments Pyris-1 DSC, PS sample, $m_{\mathrm{s}} = 25$ mg with standard aluminum pan of about 25 mg.

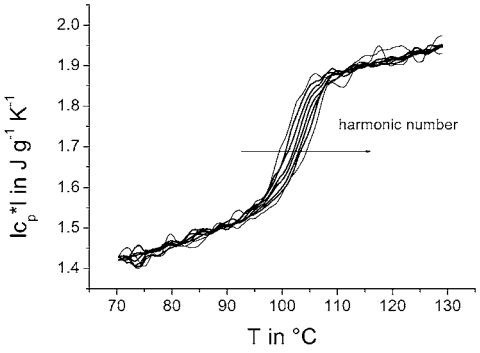

Fig. 13. Modulus of specific heat capacity of PS vs. temperature for 1st, 2nd, 3rd, 5th, 7th, 10th, 15th and 21st harmonics. Experimental conditions as in Figs. 11 and 12.

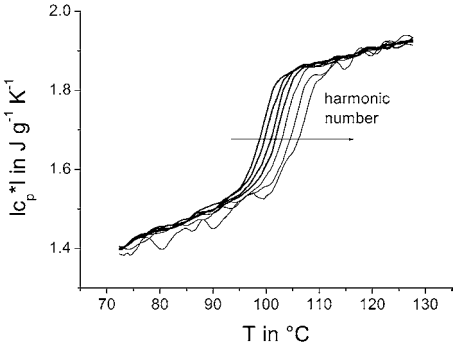

Fig. 14. Modulus of specific heat capacity of PS vs. temperature for 1st, 2nd, 4th, 8th, 16th, 32nd, 64th harmonics. Perkin-Elmer Instruments Pyris-1 DSC, PS sample, $m_s = 25$ mg, $t_p = 20$ min.

smaller after the sample was vitrified (after about 300 min, i.e. below 100°C).

Further we calculated the effective heat capacity by Eq. (9) and applied the advanced calibration algorithm, described in [13] to get the correct value of complex specific heat capacity c_p^*. The result for modulus of c_p^* is shown in Fig. 13.

We had to use an intercooler to keep the DSC block at low temperatures ($T_{block} = -50$°C) to be able to realize the fast cooling rate. Sample run and empty-pan run did not optimally correspond to each other because of ice formation during changing the sample. Due to this reason the quality of the results shown in Fig. 13 is not the best that one can achieve with the instrument. Therefore, we performed another measurement, this time with warm block ($T_{block} = 5$°C) using heating steps. The temperature–time profile was programmed by repeating isotherm and fast heating segments. The duration of the isotherm was 20 min and the heating step was 2 K high (again to keep linear conditions for the instrument) with 150 K min^{-1} heating rate that makes duration of the heating segment 0.8 s.

The result is shown in Fig. 14 (modulus of c_p^*) and Fig. 15 (phase angle of c_p^*). $c_p^*(\omega)$ at 64th harmonic is noisier than lower harmonics because corresponding heating rate amplitude is smaller.

Out of the glass transition region heat capacity is real valued and shows no frequency dependence within experimental uncertainties. At glass transition heat capacity is complex and frequency dependent. Glass transition temperature T_g is determined by the position of the half step in modulus of c_p^* or by the maximum of the imaginary part of c_p^*, which practically corresponds to the maximum of the phase angle, Arg(c_p^*). Both results for modulus and phase angle of c_p^* show the typical dynamic glass transition curves for PS — the position of T_g is shifted for about 3.5 K to higher temperature by increasing frequency for one order of magnitude [14,15], see Fig. 16.

5.2. Reversible melting of polyethylene oxide

Polyethylene oxide (PEO) was chosen as an example of complicated melting behavior because it shows enormous reorganization during step-wise heating through the melting region.

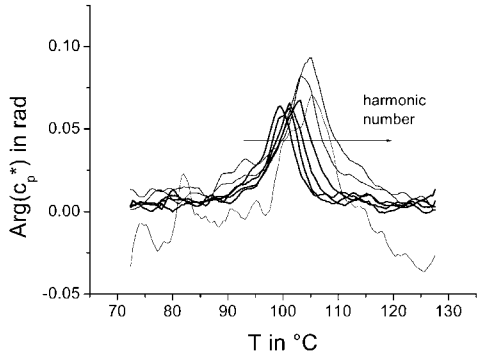

Fig. 15. Argument of specific heat capacity of PS vs. temperature for 1st, 2nd, 4th, 8th, 16th, 32nd, 64th harmonics. Perkin-Elmer Instruments Pyris-1 DSC, PS sample, $m_s = 25$ mg, $t_p = 20$ min.

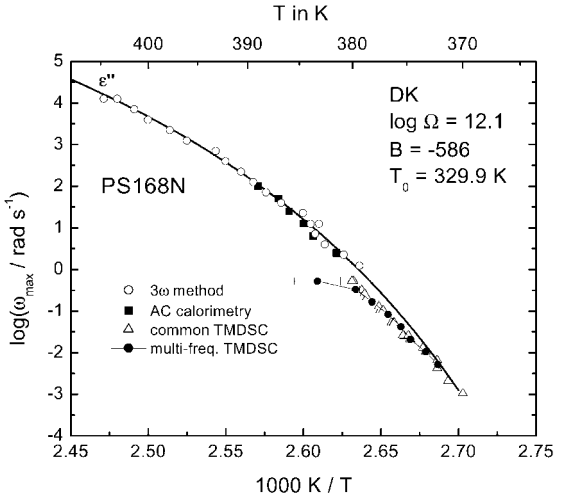

Fig. 16. Activation diagram for PS. Data from 3ω method, AC calorimetry and common TMDSC were taken from [14,15]. We added the points from the multi-frequency measurement for 1st, 2nd, 4th, 8th, 16th, 32nd, 64th and 100th harmonics, closed circles. Even at 100th harmonic one can still detect glass transition, however with large uncertainties, as indicated by the error bar. Perkin-Elmer Instruments Pyris-1 DSC, PS sample, $m_s = 25$ mg, $t_p = 20$ min.

The temperature–time program for each quasi-isotherm had three modulations. This time we took a rectangular temperature profile consisted of 5 min isotherm, cooling for 1 K at 150 K min^{-1}, 5 min isotherm, heating for 1 K at 150 K min^{-1} and so on, see insert in Fig. 17. Note again that at this temperature amplitude the instrument responds linearly, see Section 4. After three oscillations the sample was heated to the next quasi-isotherm (to the next mean temperature $T_{\text{quasi-isotherm}}$).

After heating to the next mean temperature the c_{eff} value relaxes with time. We presented the values at the middle of each quasi-isothermal measurement. The results for the absolute value of the effective heat capacity c_{eff} are shown in Fig. 17. From such measurement one can detect up to 101st or even higher harmonic in the heat flow (corresponding modulation period of 6 s or less). But to get the correct absolute c_p^* value out of 101st harmonic would be difficult. Therefore, we did not plot such high harmonics in the figure. At each particular frequency the modulus of heat capacity increased with increasing temperature until 64°C. At the next heating to 66°C the sample melted completely and c_{eff} dropped down to the value of c_p of

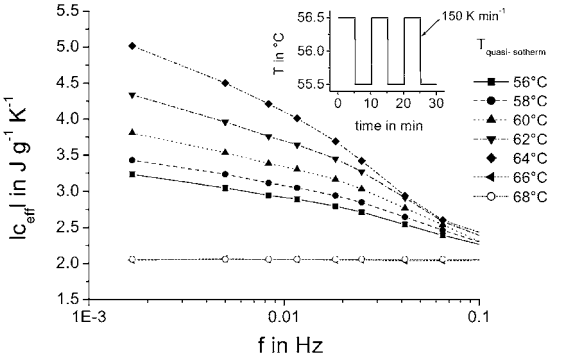

Fig. 17. Modulus of c_{eff} vs. frequency of temperature oscillations for different mean temperatures $T_{\text{quasi-isotherm}}$. Perkin-Elmer Instruments Pyris-1 DSC, PEO sample, $m_s = 11$ mg, 1 K peak-to-peak temperature amplitude, $t_p = 10$ min. The insert shows the temperature–time program for the first quasi-isotherm.

the melt, which shows no frequency dependence and almost the same values for 66 and 68°C.

We do not recommend to take these data as reference for other analogous measurements where the thermal history could be different. But what we want to show is that at a given quasi-isotherm between 56 and 64°C the modulus of c_{eff} monotonously decreased with harmonic number, i.e. with frequency of temperature oscillations. There is no appreciable scatter in modulus, because all c_{eff} values were taken simultaneously at the same moment for the same thermal history of the sample.

6. Discussions

The most important prerequisite of dynamic heat capacity determination is linear and stationary response. Without that any TMDSC result is uncertain. As we see on the examples the whole detectable heat flow spectrum is not distorted by the instrument. It means that instrumental response is highly linear and stationary. The multi-frequency method works surprisingly good in the glass transition region. Just at glass transition the thermal response is non-linear which leads to harmonic distortions [11]. One expects that harmonic distortions will interfere with the higher harmonics we are looking at. But in reality higher harmonics induced by the rich spectrum of heating rate (linear part of the sample response) are much larger than the harmonic distortions. That is why the

method works and the results were just as expected from dynamic measurements at single frequencies.

To have the same material properties for all measurements at different frequencies may appear not to be a big issue at glass transition, since the thermal history often can be easily reproduced. But the situation in the melting region is quite different because material properties change a lot and often in an irreproducible way. For example at a given mean temperature the $c_{\mathrm{eff}}(\omega)$ value can relax with time. It makes difficult the comparison of the results at different frequencies measured common way, since measurements must be performed one after another. One needs additional assumptions, i.e. that the $c_{\mathrm{eff}}(\omega)$ values relax similarly for all measured frequencies [5]. To repeat the same thermal history is also difficult. Only a multi-frequency approach can guaranty an exact correspondence of the sample history for all frequencies.

Another advantage of simultaneous multi-frequency measurements is time saving and saving of samples. For example by studying dynamic glass transition of amorphous metals the sample inevitably crystallizes once heated above the glass transition temperature. To measure the glass transition next time at another frequency would be impossible with the same sample. Only a multi-frequency approach can deliver the necessary heat capacity spectrum in a single run.

Not only TMDSC is used to perform simultaneous multi-frequency measurements of dynamic heat capacity. In [16] the technique called "Fourier transform thermal analysis" is presented where a square pulse heat flow profile is applied to a thin film and higher harmonics up to 42nd in temperature are observed. Since the heat flow profile is rectangular, it corresponds to a rectangular heating rate profile. Therefore, temperature amplitude decreases very fast with harmonic number. However, one can apply heat pulses close to ideal delta functions to generate richer temperature spectrum. Of course it is impossible to apply very sharp cooling pulses, but it is neither necessary. Heating pulses alone will generate a temperature profile like shown in Figs. 1 and 2.

7. Conclusion

We presented a method for simultaneous multi-frequency heat capacity measurements by TMDSC. The temperature–time profile for these measurements should contain sharp steps. This is the key to measure simultaneously heat flow rate at all harmonics as good as possible. The method provides good results even when the sample response in non-linear (quasi-linear), like at glass transition. Under temperature–time profiles consisting of temperature steps the instrument automatically deliver the whole heat capacity spectrum available. Only the lower part of the spectrum is cut at the basic frequency. The results are independent on the direction of temperature changes (sharp cooling or sharp heating steps or both of them in a rectangular temperature profile). Under limiting cooling possibility sharp heating steps alone are preferable. If only a couple of lower harmonics are of interest, it is absolutely unimportant that all other harmonics remain unconsidered. Their presence does not influence the results. For instruments with limited cooling capabilities asymmetric saw-tooth (fast heating and slow cooling) yields better signal-to-noise ratio than sinusoidal temperature modulation. For many DSC instruments which do not have TMDSC features with sinusoidal modulation these temperature–time profiles can be more preferable and easier to program.

Acknowledgements

This work was financially supported by Perkin-Elmer Instruments, USA. The authors gratefully acknowledge fruitful discussions with B. Wunderlich.

References

[1] H. Gobrecht, K. Hamann, G. Willers, J. Phys. 4 (1971) 21.
[2] M. Reading, Trends Polym. Sci. 8 (1993) 248.
[3] A. Boller, C. Schick, B. Wunderlich, Thermochim. Acta 266 (1995) 97.
[4] A. Toda, T. Oda, M. Hikosaka, Y. Saruyama, Thermochim. Acta 293 (1997) 47.
[5] M. Merzlyakov, A. Wurm, M. Zorzut, C. Schick, J. Macromol. Sci.-Phys. 38 (1999) 1045.
[6] W. Hu, T. Albrecht, G. Strobl, Macromolecules 22 (1999) 7548.
[7] B. Wunderlich, R. Androsch, M. Pyda, Y.K. Kwon, Thermochim. Acta 348 (2000) 181.
[8] R. Androsch, B. Wunderlich, Thermochim. Acta 333 (1999) 27.

[9] W. Hemminger, G. Höhne, Calorimetry, Verlad Chemie, Weinheim, 1984.
[10] M. Merzlyakov, C. Schick, Thermochim. Acta 330 (1999) 55.
[11] C. Schick, M. Merzlyakov, A. Hensel, J. Chem. Phys. 111 (1999) 2695.
[12] M. Merzlyakov, C. Schick, J. Thermal Anal. Cal. 61 (2000) 649.
[13] G.W.H. Höhne, M. Merzlyakov, C. Schick, Paper on Calibration, part II, this issue.
[14] S. Weyer, A. Hensel, J. Korus, E. Donth, C. Schick, Thermochim. Acta 304/305 (1997) 251.
[15] H. Huth, M. Beiner, S. Weyer, M. Merzlyakov, C. Schick, E. Donth, this issue.
[16] J. Morikawa, T. Hashimoto, Jpn. J. Appl. Phys. 37 (1998) L1484.